

## RESEARCH ARTICLE

View Article Online  
View Journal | View IssueCite this: *Org. Chem. Front.*, 2025, 12, 4321

# Aromaticity switch of borabenzene: from aromatic when free or weakly aromatic when fused to 2D PAHs to non-aromatic when fused to 3D carboranes†

Zahra Noori <sup>a</sup> and Jordi Poater <sup>\*a,b</sup>

Free borabenzene is aromatic, but when fused with 3D aromatic carborane, it loses its aromaticity. A new series of *ortho*-carborane-fused boracycles has been successfully synthesized through selective intramolecular C–H borylation, with claims of forming fused 3D/2D aromatic systems. However, our quantum chemical analysis shows that while the boron cage maintains its aromatic character, the boracycle loses its aromaticity. The limited overlap between the  $\pi$  molecular orbitals of the planar boracycle and the  $n + 1$  molecular orbitals of the carborane hinders significant electronic delocalization between the two fused components. Our findings reveal that the peripheral  $\sigma$ -aromaticity of the carborane and the  $\pi$ -aromaticity of the boracycle are not fused, making a true 3D/2D aromatic system unattainable. In contrast, when the same boracycle is fused to a 2D aromatic polycyclic aromatic hydrocarbon (PAH), it retains partial aromaticity. Thus, the aromaticity of free boratabenzene is lost when fused with 3D aromatic carborane, *i.e.*, it switches from aromatic to non-aromatic when fused to carborane or weakly aromatic when fused to PAHs.

Received 7th March 2025,  
Accepted 9th April 2025

DOI: 10.1039/d5qo00449g

rsc.li/frontiers-organic

## Introduction

Boron heterocycles, a key subset of heteroatom-incorporated rings, are notable for their empty  $p_z$  orbital at the boron center, which makes them strong Lewis acids and allows for easy modulation of electronic and photophysical properties.<sup>1,2</sup> Their potential for extensive functionalization<sup>3</sup> has led to wide-ranging applications in catalysis, chemical biology, materials science, and as synthons for conjugated materials.<sup>2,4</sup> Organoboron compounds, particularly boron-containing rings or boracycles, have long been central to synthetic chemistry. With tricoordinate boron providing a Lewis acidic site, boracycles enable facile tuning of electronic structures and continue to be explored for their versatile chemical behavior, especially in their prevalent B(III) oxidation state.<sup>1</sup>

When we talk about boron heterocycles, we must first focus on the simplest boracycle, borabenzene, that can be found either as the neutral Lewis base stabilized borabenzene or the

anionic boratabenzene (Fig. 1).<sup>5</sup> With regard to the aromaticity of the neutral borabenzene, Karadakov and coworkers, by means of valence bond theory (with six active  $\pi$  orbitals and

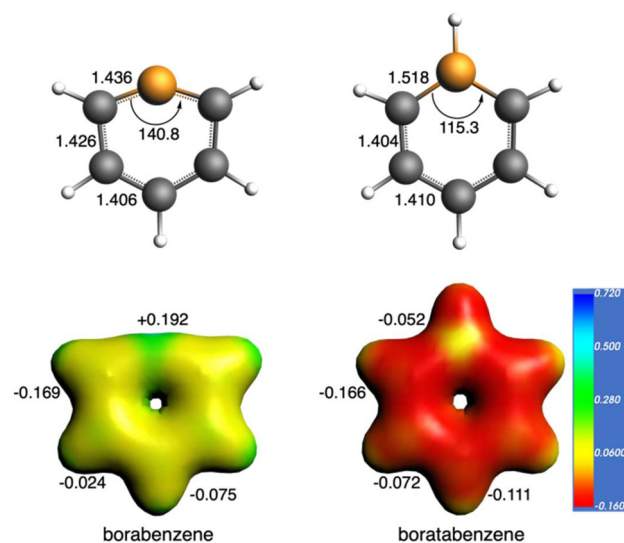


Fig. 1 Geometries of borabenzene and boratabenzene anion (top, bond lengths in Å and angles in degrees); molecular electrostatic potential isosurfaces (bottom, isovalue = 0.03) and VDD (in a.u.) of boron and carbon atoms.

<sup>a</sup>Departament de Química Inorgànica i Orgànica & Institut de Química Teòrica i Computacional (IQTCUB), Universitat de Barcelona, Martí i Franquès 1-11, 08028 Barcelona, Spain

<sup>b</sup>ICREA, Pg. Lluís Companys 23, 08010 Barcelona, Spain.

E-mail: jordi.poater@ub.edu

† Electronic supplementary information (ESI) available. See DOI: <https://doi.org/10.1039/d5qo00449g>



with four and eight active  $\sigma$  orbitals), suggested that the  $\pi$ -electron sextet in borabenzene is aromatic.<sup>6</sup> And the reactivity of the molecule likely stems from its  $\sigma$  framework,<sup>7</sup> particularly due to “bent” boron–carbon  $\sigma$  bonds that create an orbital “hole” at the boron atom, making it a preferred attachment site for Lewis acids.

On the other hand, polycyclic aromatic hydrocarbons (PAHs) have gained significant attention in the field of electronic materials due to their extended conjugation, which facilitates electron transport.<sup>8,9</sup> Traditionally, PAHs consist of 2D aromatic  $\pi$ -systems, but introducing a tricoordinate boron center into their framework can modify the frontier molecular orbitals, thereby impacting their photophysical, electronic, and magnetic properties.<sup>4,10,11</sup> Icosahedral dicarbadodecaborane clusters ( $C_2B_{10}H_{12}$ ), known for their 3D aromaticity,<sup>12–15</sup> are becoming increasingly appealing for integration into extended networks because of their high stability and electron-withdrawing nature when bound to carbon atoms.<sup>11,16</sup> The incorporation of carboranes into extended  $\pi$ -systems is rare,<sup>17–20</sup> providing a unique opportunity to expand chemical exploration beyond conventional 2D PAHs.<sup>9,21–23</sup> Despite the few previous success in introducing a boracycle into a PAH, very recently, Martin and coworkers have successfully proven that selective intramolecular C–H borylation offers a straightforward approach to synthesize such 3D/2D fused analogs of PAHs.<sup>9</sup> Their method allows the formation of unsaturated five- and six-membered boracycles that link an arene to an *ortho*-carborane, thus giving boron-doped analogues of PAHs that are claimed to be fused 3D/2D aromatic systems.

However, we have recently demonstrated that, unlike many 2D/2D and 3D/3D aromatic fusions that maintain their aromaticity, a 3D/2D aromatic combination is not viable due to the ineffective overlap between the  $\pi$  molecular orbitals of the planar species and the  $(n + 1)$  molecular orbitals of the aromatic cage.<sup>17,18,24,25</sup> This insufficient overlap prevents efficient electronic delocalization between the two fused units. Shortly after, Kelemen and colleagues confirmed that our findings also applied to *ortho*-carboranes fused with five-membered ring systems.<sup>26,27</sup> The position of the heteroatom in these *exo* rings determines the bonding, resulting in restricted conjugation and, as a result, no aromatic stabilization. Additionally, the magnetic field generated by the 3D cluster affects the conjugation and the calculated magnetic properties of the fused *exo* ring, potentially leading to the incorrect assignment of aromatic character to this ring.<sup>17,24,27</sup>

Based on the above research, are boracycles aromatic when fused to either 2D aromatic PAHs or 3D aromatic carboranes? With the aim to better understand the aromaticity of boracycles, we have undertaken a quantum chemical study of a series of previously synthesized 3D/2D and 2D/2D systems enclosing this heterocycle. Aromaticity has been assessed by means of magnetic-, geometric-, and electronic-based criteria.<sup>28–30</sup> We will prove how the peripheral 3D  $\sigma$ -aromaticity of the boron cluster and the  $\pi$ -aromaticity of the boracycle cannot be fused, which translates into an unachievable 3D/2D aromatic system, but only the former remains aromatic.

## Results and discussion

### Borabenzene and boratabenzene anion

Let us start with the simplest boracycle, borabenzene, referred in the Introduction. We confirm that both borabenzene and boratabenzene anion are aromatic, with electronic aromaticity criterium MCI that amounts to 0.050 and 0.030 a.u., respectively (Fig. 2).<sup>5,6</sup> And the strong diatropic ring current strengths in both systems also support their aromatic character (Fig. 3). However, their aromaticity differs from one to the other, as it can already be guessed from their geometries. Whereas boratabenzene anion keeps an almost hexagonal geometry, that of borabenzene is a distorted hexagon, with a CBC angle of 140.8° (Fig. 1). In addition, the C–B bond length in borabenzene is 1.436 Å, that could be considered a double bond, whereas that in boratabenzene is 1.518 Å, typical of a single bond. This translates into a smaller bond length alternation in the former (Fig. S7†). The aromaticity of both systems is also confirmed by geometric-based HOMA values (0.687 and 0.848 a.u. for boratabenzene and borabenzene, respectively, Table S1†). Thus, both systems possess a  $\pi$ -sextet (Fig. S1†), but borabenzene presents a more delocalized structure,<sup>31–33</sup> whereas the aromaticity of boratabenzene is achieved thanks to its anionic character (VDD charges enclosed in Fig. 1), driving to the 6  $\pi$  electrons required to satisfy Hückel's  $4n + 2$  rule.

Despite the failure to synthesize free borabenzene, its adduct with pyridine has been isolated as a yellow crystalline solid.<sup>34</sup> This pyridine–borabenzene compound can be referred as a donor–acceptor complex, in which the electrons of the bond connecting the two rings are mainly provided by pyridine. The boracyclic is aromatic and, importantly, it keeps a regular hexagonal shape, *i.e.*, it behaves like boratabenzene due to the donor character of pyridine (Fig. 2). In particular, both MCI and ring current strengths are very similar to those of boratabenzene (Fig. 3). And, regarding the ring currents, both borabenzene and pyridine rings show diatropic ring currents, *i.e.*, aromatic. Thus, also in this case the 6  $\pi$  electrons to accomplish Hückel's rule of the boracyclic ring are achieved, but not as an anionic system, but due to the donor–acceptor interaction with the pyridine. In particular, the borabenzene ring adopts a total charge of  $-0.372e$ , with B slightly negatively charged ( $-0.007e$ ). And the molecular orbitals for this system also show the  $\pi$  sextet localized in this ring (Fig. S2†). Noticeably, in case of borabenzene above, the short C–B bond lengths cause hyperconjugation, thus increasing its  $\pi$ -character through in-plan  $\pi$ -overlap. However, when stabil-

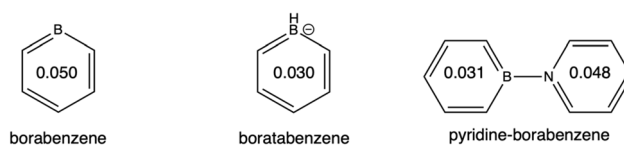
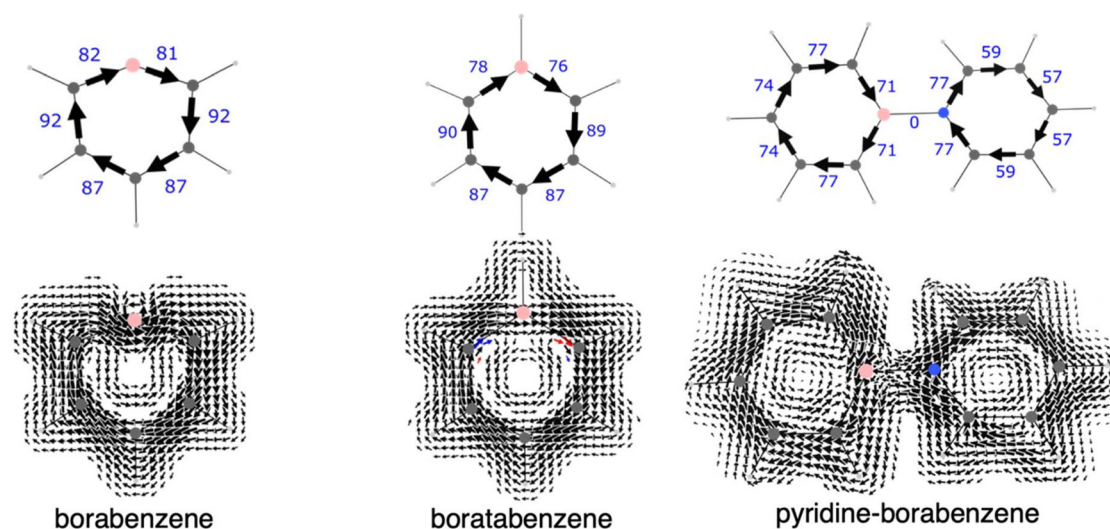


Fig. 2 MCI values (in a.u.) of borabenzene reference systems and fused cycloboranes with *o*-carborane.





**Fig. 3** Bond current strengths for a magnetic field perpendicular to the molecular plane of borabenzene reference systems. Values aside each arrow represent the percentage relationship with respect to a reference current strength of  $12 \text{ nA T}^{-1}$  (top). And current density maps (all-electron contributions) for a perpendicular magnetic field over a plane 1 a.u. below the molecular plane (bottom).

ized with pyridine, this electronic effect is switched off by direct stabilization of the outward pointing empty  $sp$  hybrid, thus offering both kinetic and thermodynamic stability that have driven to its synthesis.

### First synthesized carboranes fused to PAHs including boracycle

The first synthesized carboranes fused to boracyclic analogues of PAHs were achieved by Nie, Siebert and coworkers,<sup>21</sup> and later by Braunschweig, Marder and coworkers.<sup>22</sup> Both groups synthesized a kind of diboraanthracene (Fig. 4). With respect to their aromaticity, MCI of the boracyclic ring of both systems is 0.000 a.u., thus assigning them a non-aromatic character. This latter is further supported by the ring current strengths (Fig. 5), with an almost inexistent current, neither diatropic nor paratropic. At difference, the fused benzene rings are clearly aromatic with large MCI values (0.057 and 0.054 a.u. for Siebert and Marder systems, respectively) and strong diatropic ring currents. In case of the latter system, the 9-boraffluorene

presents two aromatic benzene rings, whereas the middle five-membered  $BC_4$  ring also presents a very small MCI value (MCI = 0.005 a.u.). At difference to the six-membered boracyclic ring fused to the *o*-carborane, this one shows a paratropic ring current (Fig. 5), arisen from the two localized diatropic ring currents of the benzene rings to which is fused. This assigns an anti-aromatic to it. Thus, we can state that these both systems by Siebert and coworkers,<sup>21</sup> and Marder and coworkers<sup>22</sup> present a 3D aromatic carborane and a 2D aromatic benzene, connected or bridged by a non-aromatic boracyclic ring.<sup>24,35–42</sup> The aromaticity of the carborane is supported by strongly negative NICS values (around  $-30$  ppm in all systems), in agreement with previous works.<sup>17,18,24,25</sup>

### 3D/2D boracyclic analogues of PAHs by Martin and coworkers

Let us now focus on the 3D/2D fused analogues of PAHs very recently synthesized by Martin and coworkers through selective intramolecular C–H borylation reactions.<sup>9</sup> For a better understanding, we have kept the same nomenclature as in their manuscript. Computed MCI values further support the non-aromaticity of the cycloborane fused to the carborane (Fig. 6, MCI = 0.000 a.u.), either as a five- (systems 1 and 2) or six-membered rings (systems 3 and 4). At difference, the PAHs attached to the boracycle are aromatic, either benzene (system 1), naphthalene (systems 2 and 3), or phenanthrene (system 4). The aromaticity of these PAHs is further supported by the ring currents strengths (Fig. 7), with strong diatropic ring currents along the referred aromatic systems. At difference, there is hardly any ring current in the boracycle of the four systems, not even paratropic. Noticeably, in case of the five-membered boracycle, it is even more difficult to reach the required  $6 \pi$  electrons for Hückel's rule taking into account that one atom is the electron-deficient B. For completeness, the current density maps (Fig. S3†) for systems 3 and 4 (those enclosing

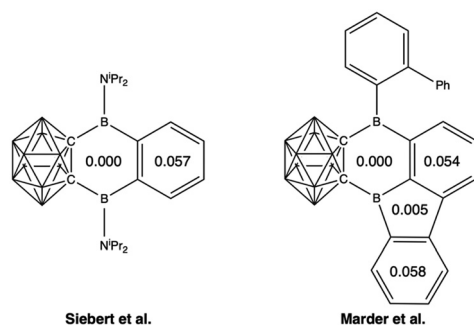


**Fig. 4** MCI values (in a.u.) of first synthesized fused cycloboranes with *o*-carborane.



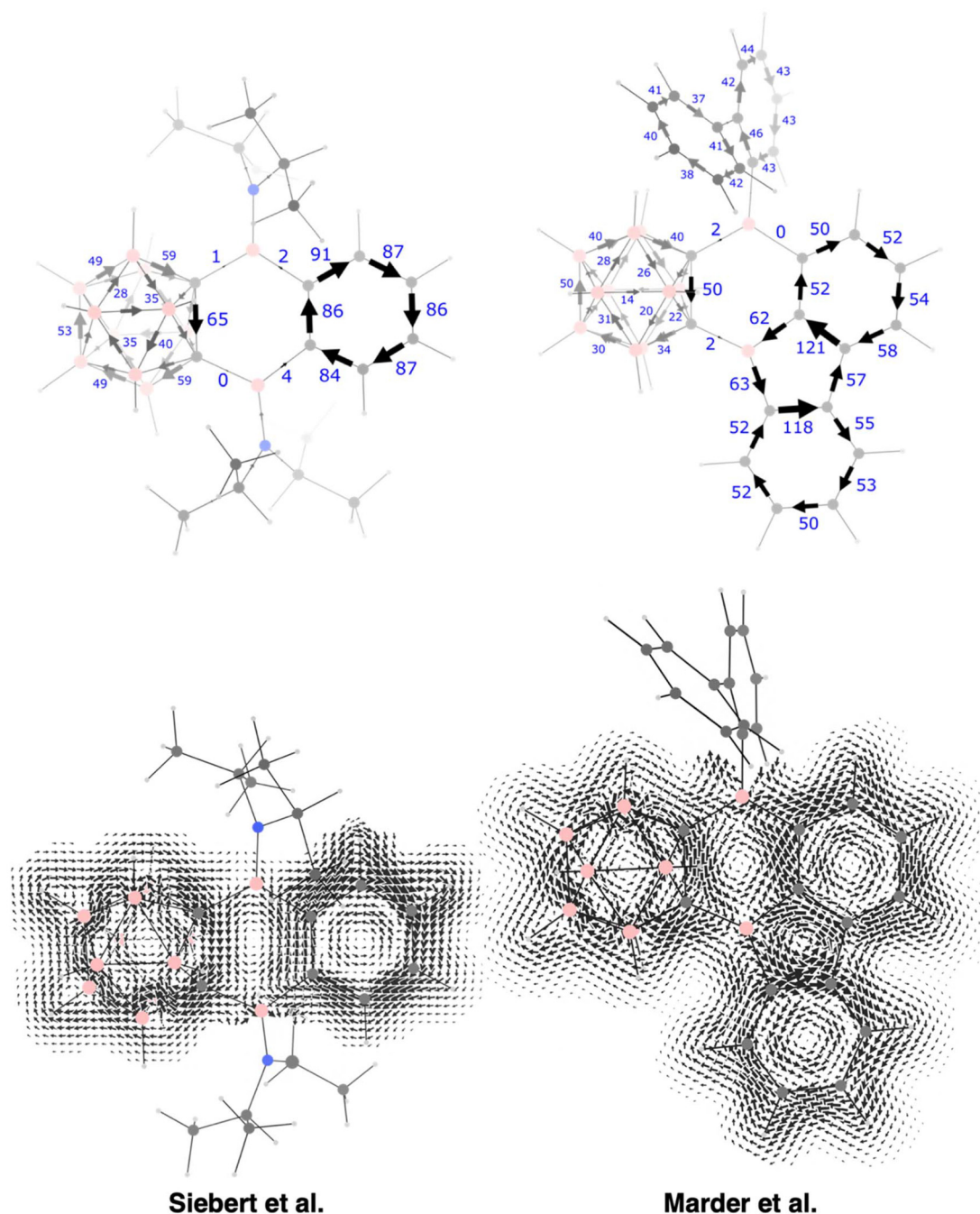


**Fig. 5** Bond current strengths for a magnetic field perpendicular to the molecular plane of first synthesized fused cycloboranes with *o*-carborane. Values aside each arrow represent the percentage relationship with respect to a reference current strength of  $12 \text{ nA T}^{-1}$  (top). And current density maps (all-electron contributions) for a perpendicular magnetic field over a plane 1 a.u. below the molecular plane (bottom).

the six-membered cycloborane) show certain coupling between the diatropic ring current around the *o*-carborane and that around the different PAHs, especially along the C–C bond connecting both units, whereas the current along the C–B–C bond is much weaker. At difference, the equivalent coupling of the diatropic ring currents for systems 1 and 2, enclosing the five-membered cycloborane, is much weaker or almost inexistent. Finally, it must be noted that systems 3 and 4, compared to

those by either Siebert or Marder above, enclose a cycloborane with only one boron atom, not two.

The above four systems previously synthesized show how the cycloborane just plays as a connector between the 3D aromatic carborane and the 2D aromatic PAHs. However, this either five- or six-membered boracycle remains as a non-aromatic ring. The same authors proposed a series of model systems (non-synthesized) for comparison of these new pro-





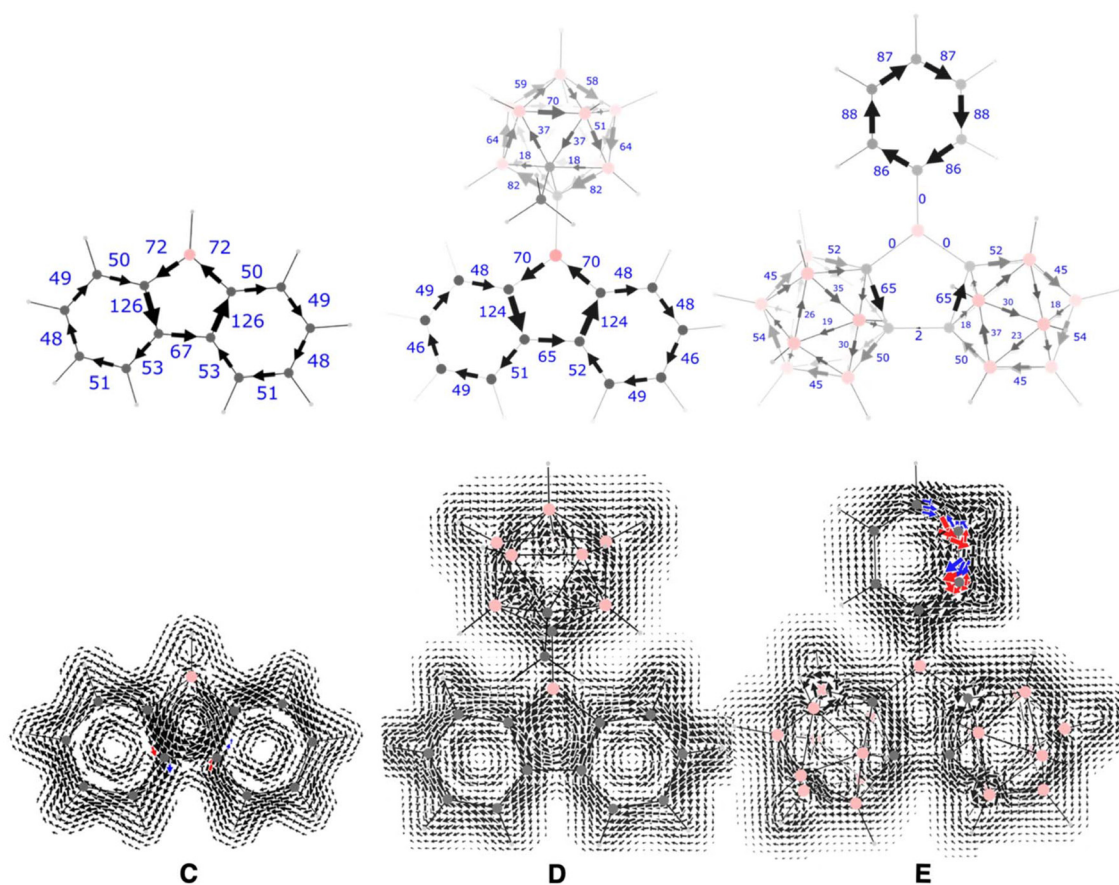


**Fig. 9** Bond current strengths for a magnetic field perpendicular to the molecular plane of model systems with fused boracyclic proposed by Martin and coworkers. Values aside each arrow represent the percentage relationship with respect to a reference current strength of  $12 \text{ nA T}^{-1}$  (top). And current density maps (all-electron contributions) for a perpendicular magnetic field over a plane 1 a.u. below the molecular plane (bottom).

rings (systems **C** and **D**), MCI slightly increases (0.005 a.u. in both cases). But, more importantly, if we focus on their ring current strengths, this boracycle adopts a paratropic ring current in both systems **C** and **D** (Fig. 9). And the reason is found in the number of  $\pi$  electrons of this five-membered ring.<sup>43,44</sup> This ring has 4  $\pi$  electrons, and thus, based on Hückel's  $4n + 2$  rule, it is antiaromatic. In particular, system **C** presents 12  $\pi$  electrons, 6  $\pi$  electrons localized in each benzene ring (Fig. S4†). The paratropic ring current in both **C** and **D** is more clearly observed in the corresponding maps (Fig. 9), much weaker in the latter due to the electron-withdrawing substituent on B, and can be compared to the absence of paratropic current in system **E**.

### 2D/2D boracyclic analogues of PAHs

We have above proven that when boracycles are fused to a 3D aromatic carborane, they cannot maintain aromaticity due to the disruption of electron delocalization caused by the dimensional transition from 2D to 3D structures. However, free borabenzene is aromatic as it has delocalized  $\pi$ -electrons following Hückel's rule ( $4n + 2$   $\pi$ -electrons). Now, let us check the case when a borabenzene (a 2D aromatic compound) is fused to other 2D aromatic rings. Fusing two 2D aromatic systems,

such as borabenzene with a typical benzene ring, could potentially preserve aromaticity, depending on the nature of the fusion and how the electrons are shared or localized between the rings. Noticeably, the set of systems under analysis have also previously been synthesized (Fig. 10).<sup>1,45–47</sup>

We first start with 1-methyl boratabenzene (system **V**) that, compared to previous boratabenzene, almost shows the same

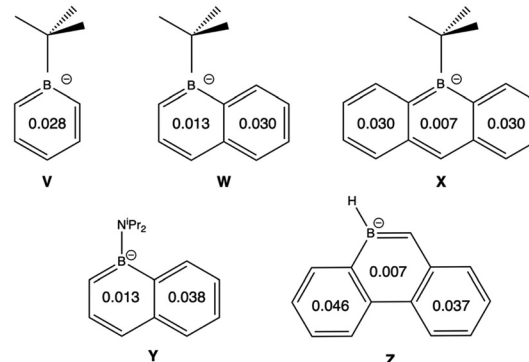


**Fig. 10** MCI values (in a.u.) of 2D/2D fused boracyclic to PAHs.



aromaticity based on MCI (0.028 a.u.). However, as soon as this system is fused to benzene (systems **W** and **Y**), its aromaticity clearly decays (MCI = 0.013 a.u.). And its aromaticity is even further reduced when fused to two benzene rings, one in each side, to either form borataanthracene (system **X**) or borataphenanthrene (system **Z**), both with MCI = 0.007 a.u. For this latter system, our MCI results would be in agreement with the work of Pino-Rios *et al.* stating that whereas the outer rings exhibit benzene-like aromaticity, the central ring is more accu-

rately considered as non-aromatic (Fig. 10).<sup>48</sup> Nonetheless, some other criteria assign to this system a similar behavior to that of phenanthrene. This is the case of the bond current strengths, that show a diatropic ring current along the periphery of all the five systems (Fig. 11). The weaker aromaticity of the cycloborane ring pointed out by MCI when going from **V** to **W**, for instance, is better observed with the corresponding current density maps. In particular, an aromatic ring shows an external diatropic ring current along the periphery of the

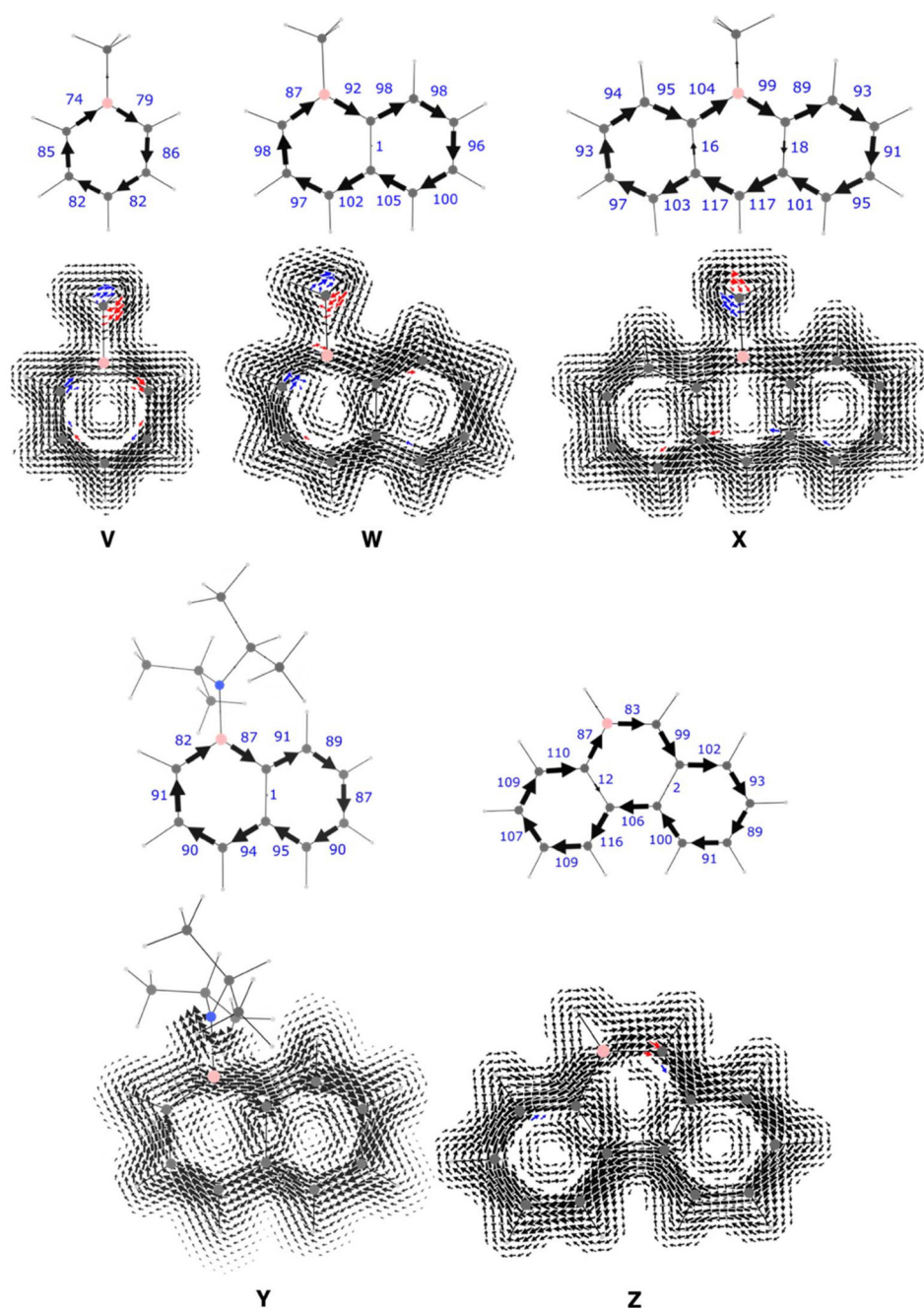


**Fig. 11** Bond current strengths for a magnetic field perpendicular to the molecular plane of 2D/2D fused boracyclic to PAHs. Values aside each arrow represent the percentage relationship with respect to a reference current strength of 12 nA T<sup>-1</sup> (top). And current density maps (all-electron contributions) for a perpendicular magnetic field over a plane 1 a.u. below the molecular plane (bottom).



atoms forming the ring, together with an internal paratropic ring current. Thus, whereas this paratropic ring current is clearly observed in **V**, the one for **W** is partially interrupted and even non-circular (Fig. 11). And such interruption in the internal paratropic ring current is even better observed in system **X**, in agreement with its even smaller MCI. The above trends are further supported by the molecular orbitals of these five systems. They allow to count the expected number of  $\pi$  orbitals to satisfy Hückel's rule. However, around the electron-deficient boron atom there is a less delocalized density (Fig. S5†).

Thus, we have observed a clear difference when the boracycle is fused to *o*-carborane versus benzene. In the former, the

boracycle becomes non-aromatic, while in the latter it remains aromatic, though less so than free borabenzene.

Finally, with the aim to further support the above statement, we have taken above analyzed systems **3** and **4**, and substituted the carborane by a benzene ring, to obtain systems **R** and **S**, respectively (Fig. 12). First, to our knowledge, these two systems have not been previously synthesized. Computed MCI amount to 0.003 a.u. for both boracycles, showing again its non-aromatic character. The added benzene in substitution of carborane is proven to be largely aromatic (MCI = 0.055 a.u.), and the same happens for the fused naphthalene in system **R** and phenanthrene in system **S**. The non-aromaticity of the boracycle is further supported by the bond current strengths (Fig. 12). We can clearly observe the diatropic ring current around the fused benzene on the left of the boracycles, as well as that around either naphthalene and phenanthrene on the right. Nonetheless, the depicted current density maps allow to see certain coupling between both diatropic ring currents in each system, although somehow interrupted next to the boron atom, thus in agreement with the current bond current strengths. For completeness, we have also studied the same systems **R** and **S**, but without the fused benzene ring, *i.e.*, systems **T** and **U**, respectively (Fig. S6†). Their MCI slightly increase to 0.006 and 0.005 a.u. for **T** and **U**, respectively, further supported by weak bond current strengths, at difference to those for either naphthalene or phenanthrene.

For completeness of the analysis of aromaticity of the above series of compounds, geometric-based HOMA has also been computed for the boracyclic ring of all systems (Table S1†). HOMA values appear to be in agreement with the trends given by both MCI and current density maps above. In addition, the depicted bond lengths of these boracyclics for all systems allow to observe the bond length alternation present in such rings, also being a prove of such lack of aromaticity (Fig. S7†).

## Conclusions

The present study highlights the fascinating interactions between 2D and 3D aromatic systems, specifically in the fusion of borabenzene and *o*-carborane. While free borabenzene maintains its aromaticity due to its  $\pi$  sextet, the fusion with 3D aromatic *o*-carborane disrupts this aromatic character. According to DFT analysis, the unavailable connection between the  $\pi$ -aromaticity of borabenzene and the  $\sigma$ -aromaticity of the carborane cage prevents electronic delocalization between the two, leading to the loss of aromaticity in the boracycle.

The electron-deficiency of boron typically necessitates electron-donor interactions to complete the  $\pi$  sextet, as seen in pyridine–borabenzene complex. However, *o*-carborane's electron-withdrawing nature and the lack of orbital overlap hinder the formation of a fused 3D/2D aromatic system in this case. Interestingly, when borabenzene is fused with benzene (another 2D aromatic system), a small degree of aromaticity

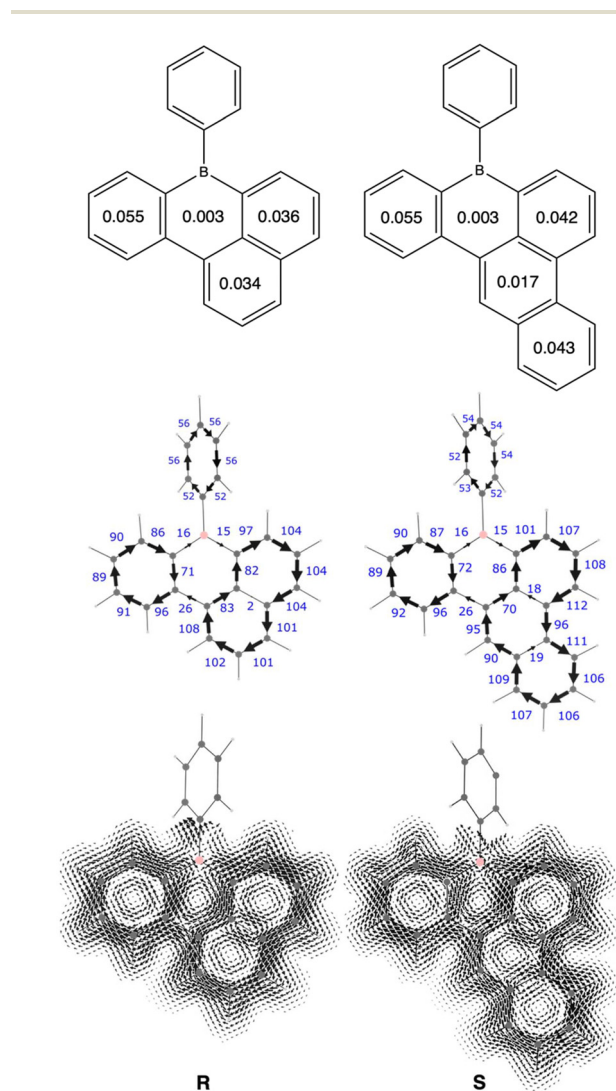


**Fig. 12** MCI values (in a.u.) of model systems 2D/2D with fused boracyclic to PAHs. Computed at ZORA-BLYP-D3(BJ)/TZ2P level of theory (top). Bond current strengths for a magnetic field perpendicular to the molecular plane. Values aside each arrow represent the percentage relationship with respect to a reference current strength of 12 nA T<sup>-1</sup> (middle). Current density maps (all-electron contributions) for a perpendicular magnetic field over a plane 1 a.u. below the molecular plane (bottom).



persists, as indicated by electronic MCI values and weak ring currents.

The study is an important step toward understanding the electronic properties of these fused aromatic systems. Ongoing research is exploring alternative heterocycles to design a fully fused 3D/2D aromatic system. This could have significant implications for materials science, particularly in the development of new electronic or optoelectronic materials.

## Theoretical methods

All calculations were performed with the AMS software<sup>49–52</sup> at the ZORA-BLYP-D3(BJ)/TZ2P level of theory. The geometry optimizations were carried out without symmetry constraints and analytical Hessians were computed to characterize the optimized structures as minima (zero imaginary frequencies). Aromaticity was first evaluated by means of the nucleus-independent chemical shift (NICS),<sup>36,38,42,53</sup> proposed by Schleyer and co-workers as a magnetic descriptor of aromaticity. NICS is defined as the negative value of the absolute shielding computed at a ring center or at some other point of the system. Rings with large negative NICS values are considered aromatic. NICS values were computed using the gauge-including atomic orbital method (GIAO).<sup>54</sup> Multicenter indices (MCI)<sup>19,20,29,55,56</sup> were computed with the ESI-3D program using AIM partition of space.<sup>57,58</sup> Current density maps have been computed by means of the SYSMOIC package<sup>59–61</sup> with the B3LYP hybrid density functional and the 6-311++G(d,p) basis set.<sup>62–64</sup> Red/blue arrows when the component parallel/antiparallel to the magnetic field **B** is greater than 30% of the vector modulus. Diatropic/paratropic circulations are clockwise/anticlockwise. Finally, a Voronoi deformation density (VDD) analysis has also been performed.<sup>65</sup>

## Data availability

Cartesian coordinates of all systems under analysis and complementary figures of the current density maps are enclosed in the ESI.†

## Conflicts of interest

There are no conflicts to declare.

## Acknowledgements

We thank Prof. Riccardo Zanasi (Salerno University, Italy) for his help and advice in the use of SYSMOIC software. We also thank the Spanish Ministerio de Ciencia, Innovación y Universidades (MCIN/AEI/10.13039/501100011033) for projects PID2022-138861NB-I00 and CEX2021-001202-M, and the Generalitat de Catalunya for project 2021SGR442. We also acknowledge CSUC for HPC facilities.

## References

- 1 K. K. Hollister, K. E. Wentz and R. J. Gilliard Jr., Redox- and Charge-State Dependent Trends in 5-, 6-, and 7-Membered Boron Heterocycles: A Neutral Ligand Coordination Chemistry Approach to Boracyclic Cations, Anions, and Radicals, *Acc. Chem. Res.*, 2024, **57**, 1510–1522.
- 2 Z. Huang, S. Wang, R. D. Dewhurst, N. V. Ignat'ev, M. Finze and H. Braunschweig, Boron: Its Role in Energy-Related Processes and Applications, *Angew. Chem., Int. Ed.*, 2020, **59**, 8800–8816.
- 3 J. Zhang and Z. Xie, A strategy for regioselective B–H functionalization of o-carboranes via base metal catalysis, *Org. Chem. Front.*, 2023, **10**, 3074–3079.
- 4 L. Ji, S. Griesbeck and T. B. Marder, Recent developments in and perspectives on three-coordinate boron materials: a bright future, *Chem. Sci.*, 2017, **8**, 846–863.
- 5 B. Su and R. Kinjo, Construction of Boron-Containing Aromatic Heterocycles, *Synthesis*, 2017, 2985–3034.
- 6 P. B. Karadakov, M. Ellis, J. Gerratt, D. L. Cooper and M. Raimondi, The electronic structure of borabenzene: Combination of an aromatic  $\pi$ -sextet and a reactive  $\sigma$ -framework, *Int. J. Quantum Chem.*, 1997, **63**, 441–449.
- 7 J. Cioslowski and P. J. Hay, Electronic structure of borabenzene and its adducts with carbon monoxide and nitrogen, *J. Am. Chem. Soc.*, 1990, **112**, 1707–1710.
- 8 Z. Sun, Q. Ye, C. Chi and J. Wu, Low band gap polycyclic hydrocarbons: from closed-shell near infrared dyes and semiconductors to open-shell radicals, *Chem. Soc. Rev.*, 2012, **41**, 7857–7889.
- 9 Y. Li, M. Tamizmani, M. O. Akram and C. D. Martin, Carborane–arene fused boracyclic analogues of polycyclic aromatic hydrocarbons accessed by intramolecular borylation, *Chem. Sci.*, 2024, **15**, 7568–7575.
- 10 W. Yang, K. E. Krantz, L. A. Freeman, D. A. Dickie, A. Molino, G. Frenking, S. Pan, D. J. D. Wilson and R. J. Gilliard Jr., Persistent Boraffluorene Radicals, *Angew. Chem., Int. Ed.*, 2020, **59**, 3850–3854.
- 11 M. O. Akram, J. R. Tidwell, J. L. Dutton, D. J. D. Wilson, A. Molino and C. D. Martin, Accessing Boron-Doped Pentaphene Analogues from 12-Boradibenzofluorene, *Inorg. Chem.*, 2022, **61**, 9595–9604.
- 12 R. Chaliha, D. S. Perumalla, K. Yadav, D. L. V. K. Prasad and E. D. Jemmis, An Extended Rudolph Diagram: B<sub>3</sub>H<sub>5</sub> and B<sub>3</sub>H<sub>6</sub><sup>+</sup> Relate 3D-, 2D-, 1D-, and 0D-Boron Allotropes, *Inorg. Chem.*, 2024, **63**, 10954–10966.
- 13 O. Shameema and E. D. Jemmis, Relative Stability of *closo-closo*, *closo-nido*, and *nido-nido* Macropolyhedral Boranes: The Role of Orbital Compatibility, *Chem. – Asian J.*, 2009, **4**, 1346–1353.
- 14 K. Vidya and E. D. Jemmis, Relative stabilities of condensed face sharing mono- and di-carboranes: CB<sub>20</sub>H<sub>18</sub> and C<sub>2</sub>B<sub>19</sub>H<sub>18</sub><sup>+</sup>, *J. Organomet. Chem.*, 2015, **798**, 91–98.
- 15 A. Muñoz-Castro, Interplay Between Planar and Spherical Aromaticity: Shielding Cone Behavior in Dual Planar-



- Planar, Planar-Spherical and Spherical-Spherical Aromatics, *ChemPhysChem*, 2020, **21**, 1384–1387.
- 16 M. O. Akram, J. R. Tidwell, J. L. Dutton and C. D. Martin, Bis(1-Methyl-ortho-Carboranyl)Borane, *Angew. Chem., Int. Ed.*, 2023, **62**, e202307040.
- 17 F. Sun, S. Tan, H.-J. Cao, C.-S. Lu, D. Tu, J. Poater, M. Solà and H. Yan, Facile Construction of New Hybrid Conjugation via Boron Cage Extension, *J. Am. Chem. Soc.*, 2023, **145**, 3577–3587.
- 18 Z. Sun, J. Zong, H. Ren, C. Lu, D. Tu, J. Poater, M. Solà, Z. Shi and H. Yan, Couple-close construction of non-classical boron cluster-phosphonium conjugates, *Nat. Commun.*, 2024, **15**, 7934.
- 19 D. Tu, J. Li, F. Sun, H. Yan, J. Poater and M. Solà, Cage–Cage– Interaction: Boron Cluster-Based Noncovalent Bond and Its Applications in Solid-State Materials, *JACS Au*, 2021, **1**, 2047–2057.
- 20 D. Tu, H. Yan, J. Poater and M. Solà, The nido-Cage– $\pi$  Bond: A Non-covalent Interaction between Boron Clusters and Aromatic Rings and Its Applications, *Angew. Chem., Int. Ed.*, 2020, **59**, 9018–9025.
- 21 Y. Nie, J. Miao, H. Wadepohl, H. Pritzkow, T. Oeser and W. Siebert, Syntheses and Characterization of o-Carboranes Containing Fused exo-Polyhedral Di- and Triboraheterocycles, *Z. Anorg. Allg. Chem.*, 2013, **639**, 1188–1193.
- 22 J. Krebs, A. Häfner, S. Fuchs, X. Guo, F. Rauch, A. Eichhorn, I. Krummenacher, A. Friedrich, L. Ji, M. Finze, Z. Lin, H. Braunschweig and T. B. Marder, Backbone-controlled LUMO energy induces intramolecular C–H activation in ortho-bis-9-borafluorene-substituted phenyl and o-carboranyl compounds leading to novel 9,10-diboraanthracene derivatives, *Chem. Sci.*, 2022, **13**, 14165–14178.
- 23 M. Zhong, J. Zhang, Z. Lu and Z. Xie, Diboration of alkenes and alkynes with a carborane-fused four-membered boracycle bearing an electron-precise B–B bond, *Dalton Trans.*, 2021, **50**, 17150–17155.
- 24 J. Poater, C. Viñas, M. Solà and F. Teixidor, 3D and 2D aromatic units behave like oil and water in the case of benzo-carborane derivatives, *Nat. Commun.*, 2022, **13**, 3844.
- 25 Z. Noori, M. Solà, C. Viñas, F. Teixidor and J. Poater, Unraveling aromaticity: the dual worlds of pyrazole, pyrazoline, and 3D carborane, *Beilstein J. Org. Chem.*, 2025, **21**, 412–420.
- 26 D. Buzsaki, M. B. Kovacs, E. Humpfner, Z. Harcsa-Pinter and Z. Kelemen, Conjugation between 3D and 2D aromaticity: does it really exist? The case of carborane-fused heterocycles, *Chem. Sci.*, 2022, **13**, 11388–11393.
- 27 Z. Kelemen, D. Buzsáki, D. Gál, Z. Harcsa-Pintér and L. Kalabay, The possible aromatic conjugation via the different edges of (car)borane clusters – Can the relationship between 3D and 2D aromatic systems be reconciled?, *Chem. – Eur. J.*, 2024, **30**, e202402970.
- 28 G. Merino, M. Solà, I. Fernández, C. Foroutan-Nejad, P. Lazeretti, G. Frenking, H. L. Anderson, D. Sundholm, F. P. Cossío, M. A. Petrukhina, J. Wu, J. I. Wu and A. Restrepo, Aromaticity: Quo Vadis, *Chem. Sci.*, 2023, **14**, 5569–5576.
- 29 F. Feixas, E. Matito, J. Poater and M. Solà, Quantifying aromaticity with electron delocalisation measures, *Chem. Soc. Rev.*, 2015, **44**, 6434–6451.
- 30 M. Solà, Aromaticity rules, *Nat. Chem.*, 2022, **14**, 585–590.
- 31 S. C. A. H. Pierrefixe and F. M. Bickelhaupt, Aromaticity: Molecular-Orbital Picture of an Intuitive Concept, *Chem. – Eur. J.*, 2007, **13**, 6321–6328.
- 32 S. C. A. H. Pierrefixe and F. M. Bickelhaupt, Aromaticity and Antiaromaticity in 4-, 6-, 8-, and 10-Membered Conjugated Hydrocarbon Rings, *J. Phys. Chem. A*, 2008, **112**, 12816–12822.
- 33 S. C. A. H. Pierrefixe and F. M. Bickelhaupt, Aromaticity in Heterocyclic and Inorganic Benzene Analogues, *Aust. J. Chem.*, 2008, **61**, 209–215.
- 34 M. Mbarki, M. Oettinghaus and G. Raabe, Quantum-chemical Ab Initio Calculations on the Donor–Acceptor Complex Pyridine–Borabenzene ( $C_5H_5N-BC_5H_5$ ), *Aust. J. Chem.*, 2014, **67**, 266–276.
- 35 J. Poater, M. Duran and M. Solà, Aromaticity Determines the Relative Stability of Kinked vs. Straight Topologies in Polycyclic Aromatic Hydrocarbons, *Front. Chem.*, 2018, **6**, 561.
- 36 J. Poater, S. Escayola, A. Poater, F. Teixidor, H. Ottosson, C. Viñas and M. Solà, Single-Not Double-3D-Aromaticity in an Oxidized Closo Icosahedral Dodecaiodo-Dodecaborate Cluster, *J. Am. Chem. Soc.*, 2023, **145**, 22527–22538.
- 37 J. Poater, M. Solà, C. Viñas and F. Teixidor, A Simple Link between Hydrocarbon and Borohydride Chemistries, *Chem. – Eur. J.*, 2013, **19**, 4169–4175.
- 38 J. Poater, M. Solà, C. Viñas and F. Teixidor,  $\pi$  Aromaticity and Three-Dimensional Aromaticity: Two sides of the Same Coin?, *Angew. Chem., Int. Ed.*, 2014, **53**, 12191–12195.
- 39 J. Poater, M. Solà, C. Viñas and F. Teixidor, Hückel's Rule of Aromaticity Categorizes Aromatic closo Boron Hydride Clusters, *Chem. – Eur. J.*, 2016, **22**, 7437–7443.
- 40 J. Poater, C. Viñas, I. Bennour, S. Escayola Gordils, M. Solà and F. Teixidor, Too Persistent to Give Up: Aromaticity in Boron Clusters Survives Radical Structural Changes, *J. Am. Chem. Soc.*, 2020, **142**, 9396–9407.
- 41 J. Poater, C. Viñas, S. Escayola, M. Solà and F. Teixidor, Pioneering the Power of Twin Bonds in a Revolutionary Double Bond Formation. Unveiling the True Identity of o-Carboryne as o-Carborene, *Chem. – Eur. J.*, 2023, **29**, e202302448.
- 42 J. Poater, C. Viñas, M. Solà and F. Teixidor, Aromaticity and Extrusion of Benzenoids Linked to [o-COSAN]-. Clar has the Answer, *Angew. Chem., Int. Ed.*, 2022, **61**, e202200672.
- 43 O. Huertas, J. Poater, M. Fuentes-Cabrera, M. Orozco, M. Solà and F. J. Luque, Local Aromaticity in Natural Nucleobases and Their Size-Expanded Benzo-Fused Derivatives, *J. Phys. Chem. A*, 2006, **110**, 12249–12258.
- 44 C. Curutchet, J. Poater, M. Solà and J. Elguero, Analysis of the Effects of N-Substituents on Some Aspects of the



- Aromaticity of Imidazoles and Pyrazoles, *J. Phys. Chem. A*, 2011, **115**, 8571–8577.
- 45 M. Ferrer, I. Alkorta, J. Elguero and J. M. Oliva-Enrich, A theoretical study of the reaction of borata derivatives of benzene, anthracene and pentacene with CO<sub>2</sub>, *Phys. Chem. Chem. Phys.*, 2023, **25**, 22512–22522.
- 46 G. E. Herberich, E. Cura and J. Ni, A new synthetic route to 2-boratanaphthalenes, *Inorg. Chem. Commun.*, 1999, **2**, 503–506.
- 47 A. J. Ashe, X. Fang and J. W. Kampf, Synthesis and Properties of 1-Substituted 1-Boratanaphthalenes, *Organometallics*, 1999, **18**, 466–473.
- 48 R. Báez-Grez and R. Pino-Rios, Borataalkene or boratabenzene? Understanding the aromaticity of 9-borataphenanthrene anions and its central ring, *New J. Chem.*, 2020, **44**, 18069–18073.
- 49 G. te Velde, F. M. Bickelhaupt, E. J. Baerends, C. Fonseca Guerra, S. J. A. van Gisbergen, J. G. Snijders and T. Ziegler, Chemistry with ADF, *J. Comput. Chem.*, 2001, **22**, 931–967.
- 50 F. M. Bickelhaupt and E. J. Baerends, in *Reviews in Computational Chemistry*, ed. K. B. Lipkowitz and D. B. Boyd, Wiley-VCH, New York, 2000, vol. 15, pp. 1–86.
- 51 P. Vermeeren, T. A. Hamlin and F. M. Bickelhaupt, Chemical reactivity from an activation strain perspective, *Chem. Commun.*, 2021, **57**, 5880–5896.
- 52 P. Vermeeren, S. C. C. van der Lubbe, C. Fonseca Guerra, F. M. Bickelhaupt and T. A. Hamlin, Understanding chemical reactivity using the activation strain model, *Nat. Protoc.*, 2020, **15**, 649–667.
- 53 Z. F. Chen, C. S. Wannere, C. Corminboeuf, R. Puchta and P. v. R. Schleyer, Nucleus-independent chemical shifts (NICS) as an aromaticity criterion, *Chem. Rev.*, 2005, **105**, 3842–3888.
- 54 K. Wolinski, J. F. Hinton and P. Pulay, Efficient Implementation of the Gauge-Independent Atomic Orbital Method for NMR Chemical-Shift Calculations, *J. Am. Chem. Soc.*, 1990, **112**, 8251–8260.
- 55 P. Bultinck, R. Ponec and S. Van Damme, Multicenter bond indices as a new measure of aromaticity in polycyclic aromatic hydrocarbons, *J. Phys. Org. Chem.*, 2005, **18**, 706–718.
- 56 E. Matito, M. Duran and M. Solà, The aromatic fluctuation index (FLU): A new aromaticity index based on electron delocalization, *J. Chem. Phys.*, 2005, **122**, 014109.
- 57 E. Matito, ESI-3D: Electron Sharing Indices Program for 3D Molecular Space Partitioning, 2006.
- 58 E. Matito, M. Solà, P. Salvador and M. Duran, Electron sharing indexes at the correlated level. Application to aromaticity calculations, *Faraday Discuss.*, 2007, **135**, 325–345.
- 59 G. Monaco, F. F. Summa and R. Zanasi, Program Package for the Calculation of Origin-Independent Electron Current Density and Derived Magnetic Properties in Molecular Systems, *J. Chem. Inf. Model.*, 2021, **61**, 270–283.
- 60 G. Monaco, F. F. Summa and R. Zanasi, Atomic size adjusted calculation of the magnetically induced current density, *Chem. Phys. Lett.*, 2020, **745**, 137281.
- 61 R. J. F. Berger, G. Monaco and R. Zanasi, On the topology of total and diamagnetic induced electronic currents in molecules, *J. Chem. Phys.*, 2020, **152**, 194101.
- 62 A. D. Becke, Density-Functional Thermochemistry .3. The Role of Exact Exchange, *J. Chem. Phys.*, 1993, **98**, 5648–5652.
- 63 C. T. Lee, W. T. Yang and R. G. Parr, Development of the Colle-Salvetti Correlation-Energy Formula into a Functional of the Electron-Density, *Phys. Rev. B: Condens. Matter Mater. Phys.*, 1988, **37**, 785–789.
- 64 P. J. Stephens, F. J. Devlin, C. F. Chabalowski and M. J. Frisch, *Ab initio* Calculation of Vibrational Absorption and Circular-Dichroism Spectra Using Density-Functional Force-Fields, *J. Phys. Chem.*, 1994, **98**, 11623–11627.
- 65 C. Fonseca Guerra, J.-W. Handgraaf, E. J. Baerends and F. M. Bickelhaupt, Voronoi deformation density (VDD) charges: Assessment of the Mulliken, Bader, Hirshfeld, Weinhold, and VDD methods for charge analysis, *J. Comput. Chem.*, 2004, **25**, 189–210.

